HHS Public Access

Author manuscript

J Agric Food Chem. Author manuscript; available in PMC 2023 July 10.

Published in final edited form as:

J Agric Food Chem. 2023 June 07; 71(22): 8665–8672. doi:10.1021/acs.jafc.3c01946.

Engineered Yeast Displaying Specific Norovirus-Binding Nanobodies for the Concentration and Detection of Human Norovirus in Food Matrix

Xue Zhao,
Department of Biological Systems Engineering, Virginia Tech, Blacksburg, Virginia 24061, United States

Mahbubur Rahman,
Department of Biological Systems Engineering, Virginia Tech, Blacksburg, Virginia 24061, United States

Zhiyuan Xu,
Department of Biological Systems Engineering, Virginia Tech, Blacksburg, Virginia 24061, United States

Tom Kasputis,
Department of Biological Systems Engineering, Virginia Tech, Blacksburg, Virginia 24061, United States;

Yawen He,
Department of Biological Systems Engineering, Virginia Tech, Blacksburg, Virginia 24061, United States

Lijuan Yuan,
Department of Biomedical Sciences and Pathobiology, Virginia-Maryland College of Veterinary Medicine, Virginia Tech, Blacksburg, Virginia 24061, United States

R. Clay Wright,
Department of Biological Systems Engineering, Virginia Tech, Blacksburg, Virginia 24061, United States;

Juhong Chen
Department of Biological Systems Engineering, Virginia Tech, Blacksburg, Virginia 24061, United States

Corresponding Author: **Juhong Chen** – *Department of Biological Systems Engineering, Virginia Tech, Blacksburg, Virginia 24061, United States;* Phone: 540-231-1689; jhchen@vt.edu; Fax: 540-231-3199.

Author Contributions

X.Z.: investigation, methodology, and writing—original draft; M.R.: investigation and methodology; Z.X., T.K., and Y.H.: investigation; C.W.: conceptualization, project administration, supervision, methodology, materials, and writing—review and editing; L.Y., conceptualization and writing—review and editing; J.C.: conceptualization, project administration, funding acquisition, supervision, and writing—review and editing.

Supporting Information

The Supporting Information is available free of charge at https://pubs.acs.org/doi/10.1021/acs.jafc.3c01946.
Details of the codon-optimized sequence of nanobody and the primers used in this study (PDF)

Complete contact information is available at: https://pubs.acs.org/10.1021/acs.jafc.3c01946

The authors declare no competing financial interest.

Abstract

Human noroviruses pose grave threats to public health and economy. In this study, we genetically engineered yeast (*Saccharomyces cerevisiae* EBY100) to display specific norovirus-binding nanobodies (Nano-26 and Nano-85) on cell surface to facilitate the concentration of noroviruses for improved detection. Binding of norovirus virus-like particles (VLPs) to these nanobody-displaying yeasts was confirmed and characterized using confocal microscopy and flow cytometry. The ability of our engineered yeasts to capture norovirus VLPs can reach up to 91.3%. Furthermore, this approach was applied to concentrate and detect norovirus VLPs in a real food matrix. A wide linear detection range ($1-10^4$ pg/g) was observed, and the detection limit on spiked spinach was calculated as low as 0.071 pg/g. Overall, our engineered yeasts could be a promising approach to concentrate and purify noroviruses in food samples for easy detection, which allows us to prevent the spread of food-borne virus in the food supply chain.

Keywords

norovirus; engineered yeast; nanobody; virus detection; fresh produce; food safety

INTRODUCTION

Human norovirus has been recognized to be the leading cause of viral gastroenteritis and food-borne illness worldwide.[1] Each year, norovirus is responsible for almost 20 million illnesses in the United States, which contributes to more than $5.5 billion in economic losses each year.[2] Human norovirus can be found in a wide range of food products, but the food vehicles most frequently associated with norovirus outbreaks are leafy vegetables, soft fruits, and shellfish.[3,4] Norovirus can infect individuals at a minimal infectious dose of 10−100 virus particles, causing clinical symptoms of diarrhea, vomiting, fever, and abdominal pain.[5] There are currently no available vaccines or antiviral treatments for human norovirus.[6] Thus, it is crucial to develop early and rapid detection strategies for human noroviruses to prevent the spread of the virus in the food supply chain.

To detect human norovirus rapidly and sensitively in food matrices, the viruses must be concentrated and purified before detection. However, it has been a major challenge for decades to concentrate human noroviruses effectively and efficiently in food matrices. The traditional nonspecific concentration methods have the major drawback of concentrating multiple inhibitors of downstream detection, which is especially problematic in polymerase chain reaction (PCR)-based detection of human noroviruses. To specifically concentrate human noroviruses from complex food samples, the concept of using ligands (e.g., antibodies and aptamers) to specifically bind human noroviruses has gained attention because it allows for washing away of sample matrix inhibitors.[7–9] However, the high cost, batch-to-batch variation, and instability in nonbiological conditions make antibodies less pragmatic in food and agriculture systems for the separation of human norovirus.[10,11] Aptamers are linear polymers (typically DNA) with a secondary and tertiary structure displaying affinity toward a particular analyte. Compared to antibodies, aptamers represent a biorecognition element with a low cost and potentially high binding affinity. Unfortunately, the secondary structure of nucleic acids is configured solely by hydrogen bonding and is

therefore highly influenced by both intrinsic and extrinsic factors in the sample matrix.[12,13] Subtle changes in temperature, salt concentration, or pH could reduce affinity and make aptamers ineffective for biorecognition. Therefore, a novel type of ligand with improved characteristics is urgently demanded.

Nanobodies, single-domain antibodies derived from camelids and sharks,[14] are a promising type of virus-binding ligand. Although nanobodies are single-domain binders, they interact with their targets with nanomolar affinity and are easily generated to target any pathogens. Compared to antibodies and aptamers, nanobodies exhibit several unique and specific advantages, including small size, high solubility, resistance to chemical and thermal denaturation, and stability in stringent conditions.[15,16] Moreover, due to their simple structure and low complexity, nanobodies have excellent expression yield in bacteria and yeast.[17] Due to these superior features, nanobodies are considered as potential detection probes for a variety of targets, including biomarkers, bacteria, and viruses.[18] Recently, nanobodies that have a strong affinity for human norovirus have been successfully recovered from immune libraries using phage display.[19,20]

Yeast can be engineered to display nanobodies as fusions to cell surface-associated proteins and can be produced in large quantities in a low-cost manner. The cell surface is a functional interface between the inside and outside of the cell. Engineering the cell surface to display specific ligands, termed surface display systems, is attractive for many applications in microbiology and molecular biology.[21] Yeast surface display relies on an intimate linkage between the genotype (plasmid encoding the gene) and phenotype (protein scaffold expressed on the yeast cell surface).[22] Though the phage display systems have traditionally been used for the selection and screening of nanobodies and are well-established for this purpose, nanobody expression on phage-displayed systems is less efficient than that based on the yeast-displayed systems. Taking the most commonly used filamentous M13 bacteriophage as an example, each engineered M13 phage can only display 3−5 copies of nanobody fused to the N-terminus of capsid pIII.[23] As a comparison, the larger surface area available on yeast cells and the eukaryotic machinery-mediated expression allow for greater expression levels and higher yields of nanobodies for downstream applications. As reported, the display level of nanobodies on the yeast surface is variable but has been estimated at approximately 10^4–10^5 copies per cell.[24–26] Moreover, displaying nanobodies on yeast is additionally advantageous because yeast-display systems may offer increased stability and easier scalability. Although different yeast strains and yeast surface proteins have been used to display protein scaffolds, yeast (*Saccharomyces cerevisiae*) Aga2 protein (Aga2p) of the mating protein a-agglutinin is the most commonly used.[27] For use in foods and medicines, the safety of the surface expression system should be considered. Because of its “generally regarded as safe” (GRAS) status, the yeast surface expression system has been developed for food and pharmaceutical production.[28] In particular, the rigid structure of yeast cells makes them well suited for applications in biocatalysis and bioseparations.[29] A key to engineering yeasts to concentrate human noroviruses in food samples is to find appropriate nanobodies that can be readily engineered for yeast surface display.

In this study, we aimed to develop nanobody-displayed yeasts for the concentration and separation of human noroviruses in food matrices for easier detection. To accomplish

this, *S. cerevisiae* EBY100 was genetically engineered to separately display two nanobody candidates (Nano-26 and Nano-85) whose potential to bind human norovirus capsid has been previously verified.[20] Norovirus virus-like particles (VLPs) were captured by the engineered yeasts and detected using microscopy, flow cytometry, bicinchoninic acid assay, and sandwich enzyme-linked immunosorbent assay (ELISA). The efficiency of the two engineered yeasts to capture and detect norovirus was determined and compared in ideal conditions and a real food matrix. To the best of our knowledge, this is the first study to concentrate and detect noroviruses from food samples using engineered yeasts. This novel approach provides an opportunity to improve safety in the food industry that is amenable to high-volume manufacturing and application at a low cost.

MATERIALS AND METHODS

Materials and Reagents.

S. cerevisiae EBY100 strain was obtained from ATCC (Manassas, VA). The pCTcon2 plasmid was purchased from Addgene (#41843, Watertown, MA), and the pWL34 plasmid (pGP8G2, HIS3-integrating, strong constitutive pTDH3 expression, Golden Gate/Gateway destination vector) was previously generated by adding BsaI sites flanking the attR1/2 sites in pGP8GccdB (Addgene #83884) and removing BsaI sites from the ccdB and bla (AmpR) coding sequences through silent mutations using Gibson assembly.[30] All nanobody sequences were synthesized by Twist Bioscience (South San Francisco, CA) and are presented in Table S1. The primers used in this study were synthesized by Integrated DNA Technologies (Coralville, IA) and are listed in Table S2. All restriction enzymes were purchased from New England Biolabs (NEB, Ipswich, MA). Recombinant Norovirus GII.4VP1 virus-like particles (VLPs; ab256447) produced by the recombinant Norovirus GII.4 capsid protein VP1 was obtained from Abcam (Cambridge, MA) and used for the characterization of nanobody binding affinity. Pierce BCA protein assay kit was purchased from Thermo Fisher Scientific (Rockford, IL). Antibodies, including Anti-HA Tag Monoclonal Antibody with Dylight488 (26183) and Alexa Fluor 488 goat antimouse IgG (H+L) (A11001), were purchased from Invitrogen (Eugene, OR). The antibodies used for ELISA analysis including Antinorovirus Capsid protein VP1 antibody (ab272687) and horseradish peroxidase (HRP)-conjugated Goat Antimouse IgG H&L HRP (ab6789) were purchased from Abcam (Cambridge, MA). Other chemical reagents used in our study were analytical grade and obtained from Thermo Fisher Scientific (Waltham, MA). RNase-free water was used throughout this study.

Construction of Norovirus-Binding Nanobody Plasmids.

Plasmid assemblies were designed in DIVA (public-diva.jbei.org) using J5.[31] The coding sequences of norovirus-binding nanobodies (Nano-26 and Nano-85)[19] were ordered commercially and amplified using PCR with a set of forward and reverse primers, which add assembly junctions and BsaI restriction sites for Golden Gate Assembly.[32] The coding sequence for Aga2 with a C-terminal HA tag was amplified from pCTcon2 plasmid also with primers designed for Golden Gate Assembly. The PCR products were then purified and assembled with pWL34 plasmid using Golden Gate Assembly.[32] Assembly was conducted by a 25-cycle incubation for 3 min at 37 °C and 4 min at 16 °C, followed by a 5 min final

incubation at 50 °C and a 5 min heat inactivation at 80 °C. A negative control plasmid containing CD20 from pCTcon2 instead of a nanobody fused to Aga2 was assembled in the pWL34 backbone using Gibson Assembly.[30] The resulting plasmids were electroporated in *Escherichia coli* NEB-10β-competent cells.[33] Transformed cells were plated on LB plates supplemented with 100 μg/mL of ampicillin and incubated at 37 °C overnight. Colony PCR and gel electrophoresis were performed to verify insert sizes. Of those colonies that yielded DNA bands of expected sizes, the DNA sequences of the extracted plasmids were further confirmed using Sanger sequencing by alignment with designed sequences in ApE.[34]

Transformation of Yeast Expression Plasmids and Induction.

The recombinant plasmids were then linearized with PmeI digestion and then transformed into *S. cerevisiae* EBY100 using the LiAc/SS carrier DNA/PEG method.[35] Specifically, 240 μL of PEG 3350 (50%, w/v), 36 μL of 1 M lithium acetate, 50 μL of 2 mg/mL single-stranded (salmon sperm) carrier DNA, and digested plasmid DNA plus sterile water were mixed to make up the transformation mix. The transformation mix was added to the transformation tube containing the competent yeast pellet. The cell pellet was resuspended by vigorous vortexing. The tube was placed in an Eppendorf Thermomixer set to 42 °C and 200 rpm and incubated for 40 min. After the incubation, the tube was centrifuged at 13,000 *g* for 30 s in a microcentrifuge. The supernatant was discarded, and the pellet was resuspended in 1 mL of sterile water, centrifuged again as above, and resuspended in 50−200 μL. Yeast suspensions were plated on SDCAA-TRP (glucose, yeast nitrogen base, casamino acids, disodium phosphate, monosodium phosphate) selective plate and incubated at 30 °C for 3−4 days.

The transformed nanobody-displayed engineered yeasts were streaked on SDCAA-TRP selective media plates. Multiple colonies were subsequently inoculated into SDCAA-TRP media and incubated at 30 °C until a culture optical density OD_{600} reached 1.0. The OD_{600} value was measured by the Nanodrop 2000c Spectrophotometer (Thermo Scientific, Waltham, MA). To enhance the expression of nanobodies on yeast surface, yeast cells were 10-fold diluted in SDCAA-TRP media and incubated at 20 °C for 48 h. The engineered yeasts were washed three times in phosphate-buffered saline (PBS) and stored in PBS at 4 °C until use. Engineered yeasts with Aga2p-HA-Nano-26 and Aga2p-HA-Nano-85 fusions were named EY-NB-26 and EY-NB-85, respectively. Engineered control yeast with the CD20 peptide from pCTcon2 instead of a nanobody was termed EYpCTcon2. Positive yeast colonies were selected for colony PCR, and gel electrophoresis was performed to verify the insertion of interests.[36]

Validation of Nanobody Expression on the Engineered Yeast Surface.

To characterize the display efficiency of nanobodies on the yeast surface, immunofluorescence analysis was conducted based on the method of Guo et al. with minor modifications.[37] Briefly, 1×10^7 engineered yeast cells (EY-NB-26 and EY-NB-85) were centrifuged at 3000 *g* for 2 min and then resuspended in 200 μL of PBS with 0.5% (w/v) bovine serum albumin (BSA). Wild-type and EY-pCTcon2 yeasts were used as negative and positive controls, respectively. Cells were incubated with Alexa Fluor 488 labeled anti-HA antibodies (1 μL, 1 mg/mL) and incubated in the dark for 1 h at room temperature

with gentle shaking. The cells were washed of excess antibodies by centrifugation as above three times using PBS containing 0.5% of BSA (PBS-BSA). The pellets were resuspended in 50 μL of PBS-BSA solution, and the fluorescent labeling of these yeasts was characterized using an Attune NxT Acoustic Focusing Cytometer (Thermo Fisher Scientific, Waltham, MA) and a confocal laser scanning microscope (LSM 800, Carl Zeiss Microscopy, Thornwood, NY).

Validation of Engineered Yeast-Norovirus Binding.

To characterize the binding of norovirus and engineered yeasts, an immunofluorescence assay was performed.[37] Specifically, 5 μL of norovirus VLPs (0.54 mg/mL) was mixed with 1×10^7 engineered yeasts in 200 μL of PBS-BSA and incubated at room temperature for 1 h. The uncaptured VLPs were washed away with PBS-BSA three times and resuspended in PBS containing 0.5% of BSA. Afterward, the remaining VLPs were labeled with 1 μL of antinorovirus capsid protein VP1 antibody (1 mg/mL) and incubated at room temperature for 1 h. After washing three times with PBS-BSA, 1 μL of secondary Alexa Fluor 488 goat antimouse IgG (2 mg/mL) was added, and the mixture was incubated for 1 h at room temperature. Excess antibodies were removed by washing with PBS-BSA. The resulting complexes were tested using flow cytometry and confocal microscopy with suitable excitation and emission filters. Wild-type yeast was used as a negative control.

Determination of Capture Efficiency (CE).

The capture efficiency was expressed as the concentration of captured norovirus VLPs divided by the original concentration of VLPs, where the concentrations of VLPs in the solution before and after separation were determined using a Pierce BCA protein assay kit.[38] Briefly, engineered yeasts were resuspended in PBS-BSA. The wild-type yeast was used as a negative control. Norovirus VLPs at different concentrations were added to yeast solutions and incubated at room temperature for 1 h. Afterward, the supernatant was collected and mixed with a BCA working reagent. The developed color solution was subject to the following absorbance measurement at 562 nm. The concentrations of VLPs (no yeast added) and uncaptured VLPs in the supernatant were calculated based on the standard BSA curve. The capture efficiency was expressed as the concentration of captured VLPs divided by the original concentration of VLPs. The capture efficiency (CE) was determined using the equation

$$\mathrm{CE}(\%) = \left(1 - \frac{C_{\text{VLPs in supernatant}}}{C_{\text{original VLPs}}}\right) \times 100 \quad (1)$$

Detection of Norovirus VLPs in Spinach Leaves.

ELISA was conducted to evaluate the performance of engineered yeasts for the detection of norovirus VLPs on spinach leaves. Fresh baby spinach was purchased from a local supermarket (Kroger, Blacksburg, VA). Spinach leaves were cut into 1 cm^2 pieces (around 50 mg), spotinoculated (1 μL/spot) with 5 μL of norovirus VLPs ($0-10^7$ pg/mL) to reach a final inoculum level of $0-10^6$ pg/g of spinach, and air-dried for 5 min. Afterward, spinach leaves were washed with 500 μL of PBS. Engineered yeasts were then added and incubated

at room temperature for 1 h. After sequential labeling with anti-VLP primary antibody (0.4 μg/mL) and HRP-conjugated secondary antibody (0.2 μg/mL) for 30 min in a 1.5 mL microcentrifuge tube, 3,3′,5,5′-tetramethylbenzidine (TMB) solution (0.2 g/L) containing 0.01% of hydrogen peroxide was added as the HRP substrate and the mixture was incubated at room temperature for 15 min. Afterward, 0.18 M of sulfuric acid was added as a stop solution, and the developed color solution was transferred to a 96-well microplate and measured at 450 nm using a microplate reader (Synergy HTX, BioTek, VT).

Statistical Analysis.

All of the tests were conducted with at least three replicates. Statistical analysis of data was performed using analysis of variance (ANOVA) by SPSS 25.0 (International Business Machines Co. Armonk, NY). Significant differences between pairs of means were analyzed using the least significant difference (LSD) test at a 95% confidence level. A P-value < 0.05 was regarded as significant.

RESULTS AND DISCUSSION

Construction of Nanobody-Displaying Yeasts.

The overall scheme for the development of engineered yeasts displaying nanobodies for the capture and detection of norovirus is shown in Figure 1. Two nanobodies (Nano-26 and Nano-85) previously shown to bind human noroviruses (genogroup GII.4)[20] were chosen for these initial proof-of-concept experiments for virus-binding engineered yeast. *S. cerevisiae* EBY100 expresses Aga1 proteins (Aga1p) on the whole-cell surface, serving as anchors to link Aga2p through two disulfide bridges (Figure 1a). The Aga2p-HA-nanobody fusions were integrated into *S. cerevisiae* genome by homologous recombination. Aga1p−Aga2p binding results in the tethering of nanobodies on the yeast cell surface. The nanobodies were expressed as C-terminal fusions to Aga2p.[39] A hemagglutinin (HA) tag was fused in-frame with the Aga2p coding sequence, before the viral-binding nanobodies, to quantify and characterize the expressed ligands on the yeast cell surface.[40] As shown in Figure 1b and confirmed by colony PCR using primers spanning the junction between the synthetic display construct and the TRP1 locus of the yeast genome in Figure 1c, the plasmids expressing the two nanobodies (345 bp for Nano-26 and 375 bp for Nano-85) as Aga2p-HA-nanobody fusions were integrated into *S. cerevisiae* genome. Yeast displaying CD20 from pCTcon2 (180 bp) instead of nanobody on the surface was constructed as a control. The expected bands for the protein fusions (643 bp for Aga2p-HA-pCTcon2, 814 bp for Aga2p-HA-Nano-26, and 829 bp Aga2p-HA-Nano-85) were observed (Figure 1c), and there was no band for the wild-type yeast. These results indicate that we have successfully integrated nanobody fusions into the yeast genome.

Characterization of the Expression of Nanobodies on the Engineered Yeast Surfaces.

The expressed Aga2p-HA-nanobody fusions were secreted from the cells and bound to the yeast surface via disulfide bonds between Aga1p and Aga2p. The expressed nanobodies on the yeast surface were characterized using confocal microscopy and flow cytometry, where the HA tag was labeled using fluorescently labeled anti-HA antibodies (Figure 2). Compared to the wild-type yeast, all engineered yeasts (EY-pCTcon2, EY-NB-26, and EY-

NB-85) were stained green on the cell periphery as visualized using confocal microscopy (Figure 2b), indicating that the Aga2p-HA-nanobody fusions successfully attached to the yeast surface through the disulfide bonds to Aga1p.[41] Furthermore, flow cytometry analysis was conducted for the high-resolution quantification of nanobody-displaying yeast cells from non-displaying cells.[42] As shown in Figure 2c, the differences in fluorescence signal between wild-type yeast and engineered yeasts can be clearly observed. All of the engineered yeasts had similar fluorescence intensity. Overall, all of these results indicated that nanobodies have been successfully expressed on yeast surfaces.

Characterization of the Binding between Nanobody-Displaying Yeast and Norovirus VLPs.

The two nanobodies we expressed on the yeast surface have been reported to bind a broad panel of norovirus genogroups with high affinity.[20] To confirm that the nanobodies expressed on the yeast surface bind norovirus, norovirus VLPs were used. VLPs act as a surrogate for norovirus, which share the same structure as infectious native norovirus but lack a genome.[43] Engineered yeasts displaying nanobodies on the cell surface were incubated with norovirus VLPs, while wild-type yeast and EY-pCTcon2 were used as controls. After removing unbound norovirus VLPs, anti-VLP primary antibodies and fluorescently labeled secondary antibodies were added and incubated sequentially (Figure 3a). After washing away excess antibodies, the resulting complexes were then characterized using confocal microscopy and flow cytometry.

As shown in Figure 3b, there was no green staining for the wild-type and EY-pCTcon2 yeasts, but bright green staining was observed for both engineered yeasts with nanobodies (middle panel). This demonstrates that norovirus VLPs were successfully captured by nanobodies expressed on engineered yeasts. In addition, the EY-NB-26 has a stronger fluorescence signal than EY-NB-85. Furthermore, the flow cytometric analysis (Figure 3c) showed that both engineered yeasts had stronger fluorescence intensity than the wild-type and EY-pCTcon2 yeasts, and EY-NB-26 had the strongest fluorescence signal. All of these results indicate that the nanobodies expressed on the yeast surface can capture norovirus VLPs and Nano-26 showed stronger binding. These results suggest that these engineered yeasts displaying nanobodies will be able to concentrate and purify human noroviruses from food samples.

Determination of Norovirus VLP Capture Efficiency Using Engineered Yeasts.

After confirming the efficient and functional display of two norovirus-binding nanobodies on the yeast surface, we further evaluated the ability and efficiency of our engineered yeasts to capture norovirus VLPs in the range of 7.5−50 μg/mL (Figure 4a). The capture efficiency (CE) at various norovirus VLP concentrations was calculated using eq 1 and plotted (Figure 4b). The ability of EY-NB-26 and EY-NB-85 to capture norovirus VLPs ranged from 35.9 to 91.3% and 26.4 to 74.3%, respectively. The capture efficiency of this method was comparable and even better than other capture approaches, such as ssDNA aptamer (2.5−36%), apolipoprotein H-conjugated magnetic beads (23.3−48.8%), bivalent synbody affinity ligands (approximately 10−65%), and polyamidoamine dendrimer/SA-biotin-mediated cascade-amplification immunomagnetic enrichment (44.26%).[44–47] Within this dynamic range, CE increased with increasing norovirus VLP concentration and a high

CE of over 90% was achieved by EY-NB-26 from a 50 μg/mL sample. Compared with EY-NB-85, EY-NB-26 showed a significantly higher ability to capture norovirus VLPs at the same concentration ($P < 0.05$). These results suggest that nanobody-displayed engineered yeasts, especially EY-NB-26, could be a promising tool for norovirus separation.

Detection of Norovirus VLPs on Spinach Using Engineered Yeasts.

Next, we tested the ability of the engineered yeasts to concentrate and detect human norovirus VLPs in food matrix using a sandwich ELISA. 60% of foodborne diseases are associated with the intake of norovirus contaminated green-leafy vegetables in the United States, such as lettuce, cabbage, and spinach.[48] Among leafy vegetables, spinach is always consumed raw in a salad with simple washing. As reported, 5 norovirus outbreaks were caused by spinach and one outbreak was attributed to the spinach-based salads in the United States during 1973−2012.[49] In this study, baby spinach was selected as a food model and spiked with norovirus VLPs at different concentrations. Buffer solution without any VLPs was used as a negative control. The spinach was then washed, and the yeasts (wild-type and three engineered yeasts) were incubated with the wash solution containing norovirus VLPs (Figure 5a). After washing the yeast three times to remove unbound VLPs, anti-VLP primary antibodies and HRP-labeled secondary antibodies were added to label VLPs sequentially. Afterward, TMB containing H_2O_2 was added as a colorimetric substrate of HRP.

In the presence of HRP, the TMB solution turned a yellow color after the addition of sulfuric acid as the stop solution, but there was no color change observed for the wild-type and EY-pCTcon2 yeasts (Figure 5b). The absorbance intensities of the color changes were measured at a wavelength of 450 nm (Figure 5c). Good linear relationships were obtained between absorbance intensity and concentration of VLPs in the range of $1-10^4$ pg/g for EY-NB-26 (R^2= 0.9912) and $10-5 \times 10^4$ pg/g for EY-NB-85 (R^2= 0.9889). The detection limit of 6.47 pg/g for EY-NB-85 was calculated using the mean of the control replicates plus three times the standard deviation, which corresponds to approximately 2.01×10^4 norovirus/g.[50,51] A significantly lower detection limit of 0.071 pg/g (≈218 norovirus/g of spinach) was observed for EY-NB-26. Our results indicated that our proposed engineered yeasts can be used to detect norovirus in food samples. The results suggest that engineered yeast displaying nanobodies, especially Nano-26, exhibited sensitivity to capture and detect norovirus in spinach leaves at a level (≈10.9 norovirus particles) close to the reported minimum infectious dose (10 virus particles), which signifies its potential application in concentrating and detecting norovirus in other food samples. However, using norovirus VLPs as a surrogate for norovirus also has limitations. For example, the potential of cross-reactivity between VLPs with other viruses or substances that have similar structures could result in false-positive results and reduce the specificity of the ELISA-based detection.[52] Considering that norovirus VLPs do not fully equate to norovirus, we will further test the specificality and sensitivity of our developed methods in food samples spiked with different norovirus genotypes as well as real contaminated samples in the future.

In summary, we have successfully developed engineered food-grade yeasts displaying nanobodies on the cell surface and demonstrated their effectiveness to concentrate and

purify human norovirus in food matrices. Within this system, two nanobodies (Nano-26 and Nano-85) were successfully expressed on the surface of *S. cerevisiae* and exhibited the ability to capture up to 91.3 and 74.3% of norovirus VLPs, respectively. Furthermore, engineered yeasts, especially EY-NB-26, displayed good reproducibility and high sensitivity for the detection of human norovirus in spinach leaves, with a low detection limit of 0.071 pg/g. This novel nanobody-displayed engineered yeast-based biosensor provides a simple, costeffective, and efficient strategy to concentrate and detect human norovirus in complex food matrices. This innovative method could be easily utilized for routine concentration and rapid detection of noroviruses, providing a benefit to the food industry and improving public health and safety.

Supplementary Material

Refer to Web version on PubMed Central for supplementary material.

ACKNOWLEDGMENTS

This work was supported by the USDA National Institute of Food and Agriculture (2023-67017-40044) and the NIH National Institute of General Medical Science (R35GM147069). In addition, Dr. X.Z. was supported by the Presidential Postdoctoral Fellowship at Virginia Tech.

REFERENCES

(1). Patel MM; Hall AJ; Vinjé J; Parashar UD Noroviruses: A Comprehensive Review. J. Clin. Virol 2009, 44, 1–8. [PubMed: 19084472]

(2). Hallowell BD; Parashar UD; Hall AJ Epidemiologic Challenges in Norovirus Vaccine Development. Hum. Vaccines Immunother 2019, 15, 1279–1283.

(3). Moore MD; Goulter RM; Jaykus L-A Human Norovirus as a Foodborne Pathogen: Challenges and Developments. Annu. Rev. Food Sci. Technol 2015, 6, 411–433. [PubMed: 25884284]

(4). Scharff RL State Estimates for the Annual Cost of Foodborne Illness. J. Food Prot 2015, 78, 1064–1071. [PubMed: 26038894]

(5). Khoris IM; Takemura K; Lee J; Hara T; Abe F; Suzuki T; Park EY Enhanced Colorimetric Detection of Norovirus Using In-Situ Growth of Ag Shell on Au NPs. Biosens. Bioelectron 2019, 126, 425–432. [PubMed: 30471568]

(6). Zhang M; Fu M; Hu Q Advances in Human Norovirus Vaccine Research. Vaccines 2021, 9, 732. [PubMed: 34358148]

(7). Moore MD; Escudero-Abarca BI; Suh SH; Jaykus L-A Generation and Characterization of Nucleic Acid Aptamers Targeting the Capsid P Domain of a Human Norovirus GII. 4 Strain. J. Biotechnol 2015, 209, 41–49. [PubMed: 26080079]

(8). Huang W; Samanta M; Crawford SE; Estes MK; Neill FH; Atmar RL; Palzkill T Identification of Human Single-Chain Antibodies with Broad Reactivity for Noroviruses. Protein Eng., Des. Sel 2014, 27, 339–349. [PubMed: 24946948]

(9). Kou B; Crawford SE; Ajami NJ; Czakó R; Neill FH; Tanaka TN; Kitamoto N; Palzkill TG; Estes MK; Atmar RL Characterization of Cross-Reactive Norovirus-Specific Monoclonal Antibodies. Clin. Vaccine Immunol 2015, 22, 160–167. [PubMed: 25428247]

(10). Chen J; Andler SM; Goddard JM; Nugen SR; Rotello VM Integrating Recognition Elements with Nanomaterials for Bacteria Sensing. Chem. Soc. Rev 2017, 46, 1272–1283. [PubMed: 27942636]

(11). Chen J; Duncan B; Wang Z; Wang L-S; Rotello VM; Nugen SR Bacteriophage-Based Nanoprobes for Rapid Bacteria Separation. Nanoscale 2015, 7, 16230–16236. [PubMed: 26315848]

(12). Kadioglu O; Malczyk AH; Greten HJ; Efferth T Aptamers as a Novel Tool for Diagnostics and Therapy. Invest. New Drugs 2015, 33, 513–520. [PubMed: 25637166]

(13). tefan G; Hosu O; de Wael K; Lobo-Castañón MJ; Cristea C Aptamers in Biomedicine: Selection Strategies and Recent Advances. Electrochim. Acta 2021, 376, No. 137994.

(14). Aria H; Mahmoodi F; Ghaheh HS; Faranak M; Zare H; Heiat M; Bakherad H Outlook of Therapeutic and Diagnostic Competency of Nanobodies against SARS-CoV-2: A Systematic Review. Anal. Biochem 2022, 640, No. 114546. [PubMed: 34995616]

(15). Ebrahimizadeh W; Mousavi Gargari S; Rajabibazl M; Safaee Ardekani L; Zare H; Bakherad H Isolation and Characterization of Protective Anti-LPS Nanobody against V. Cholerae O1 Recognizing Inaba and Ogawa Serotypes. Appl. Microbiol. Biotechnol 2013, 97, 4457–4466. [PubMed: 23135228]

(16). Aghamollaei H; Ghanei M; Rasaee MJ; Latifi AM; Bakherad H; Fasihi-Ramandi M; Taheri RA; Gargari SLM Isolation and Characterization of a Novel Nanobody for Detection of GRP78 Expressing Cancer Cells. Biotechnol. Appl. Biochem 2021, 68, 239–246. [PubMed: 32270531]

(17). Salvador J-P; Vilaplana L; Marco M Nanobody: Outstanding Features for Diagnostic and Therapeutic Applications. Anal. Bioanal. Chem 2019, 411, 1703–1713. [PubMed: 30734854]

(18). Zhang C; Liu Z; Bai M; Wang Y; Liao X; Zhang Y; Wang P; Wei J; Zhang H; Wang J; Wang H; Wang Y An Ultrasensitive Sandwich Chemiluminescent Enzyme Immunoassay Based on Phage-Mediated Double-Nanobody for Detection of Salmonella Typhimurium in Food. Sens. Actuators, B 2022, 352, No. 131058.

(19). Garaicoechea L; Aguilar A; Parra GI; Bok M; Sosnovtsev Sv.; Canziani G; Green KY; Bok K; Parreño V Llama Nanoantibodies with Therapeutic Potential against Human Norovirus Diarrhea. PLoS One 2015, 10, No. e0133665. [PubMed: 26267898]

(20). Koromyslova AD; Hansman GS Nanobodies Targeting Norovirus Capsid Reveal Functional Epitopes and Potential Mechanisms of Neutralization. PLoS Pathog. 2017, 13, No. e1006636. [PubMed: 29095961]

(21). Ueda M; Tanaka A Genetic Immobilization of Proteins on the Yeast Cell Surface. Biotechnol. Adv 2000, 18, 121–140. [PubMed: 14538113]

(22). Angelini A; Chen TF; Picciotto S; Yang NJ; Tzeng A; Santos MS; van Deventer JA; Traxlmayr MW; Wittrup KD Protein Engineering and Selection Using Yeast Surface Display. In Yeast Surface Display; Springer, 2015; pp 3–36.

(23). Murad H; Assaad JM; Al-Shemali R; Abbady AQ Exploiting Nanobodies in the Detection and Quantification of Human Growth Hormone via Phage-Sandwich Enzyme-Linked Immunosorbent Assay. Front. Endocrinol 2017, 8, 115.

(24). Chao G; Lau WL; Hackel BJ; Sazinsky SL; Lippow SM; Wittrup KD Isolating and Engineering Human Antibodies Using Yeast Surface Display. Nat. Protoc 2006, 1, 755–768. [PubMed: 17406305]

(25). Helma J; Cardoso MC; Muyldermans S; Leonhardt H Nanobodies and Recombinant Binders in Cell Biology. J. Cell Biol 2015, 209, 633–644. [PubMed: 26056137]

(26). Salema V; Fernández LÁ *Escherichia coli* Surface Display for the Selection of Nanobodies. Microb. Biotechnol 2017, 10, 1468–1484. [PubMed: 28772027]

(27). Xu G; Tasumi S; Pancer Z Yeast Surface Display of Lamprey Variable Lymphocyte Receptors. In Immune Receptors; Springer, 2011; pp 21–33.

(28). Samuelson P; Wernérus H; Svedberg M; Ståhl S Staphylococcal Surface Display of Metal-Binding Polyhistidyl Peptides. Appl. Environ. Microbiol 2000, 66, 1243–1248. [PubMed: 10698802]

(29). Shigechi H; Uyama K; Fujita Y; Matsumoto T; Ueda M; Tanaka A; Fukuda H; Kondo A Efficient Ethanol Production from Starch through Development of Novel Flocculent Yeast Strains Displaying Glucoamylase and Co-Displaying or Secreting α-Amylase. J. Mol. Catal. B: Enzym 2002, 17, 179–187.

(30). Gibson DG; Young L; Chuang R-Y; Venter JC; Hutchison CA; Smith HO Enzymatic Assembly of DNA Molecules up to Several Hundred Kilobases. Nat. Methods 2009, 6, 343–345. [PubMed: 19363495]

(31). Hillson NJ; Rosengarten RD; Keasling JD J5 DNA Assembly Design Automation Software. ACS Synth. Biol 2012, 1, 14–21. [PubMed: 23651006]

(32). Engler C; Gruetzner R; Kandzia R; Marillonnet S Golden Gate Shuffling: A One-Pot DNA Shuffling Method Based on Type IIs Restriction Enzymes. PLoS One 2009, 4, No. e5553. [PubMed: 19436741]

(33). Kurosawa K; Plassmeier J; Kalinowski J; Rückert C; Sinskey AJ Engineering L-Arabinose Metabolism in Triacylglycerol-Producing Rhodococcus Opacus for Lignocellulosic Fuel Production. Metab. Eng 2015, 30, 89–95. [PubMed: 25936337]

(34). Davis MW; Jorgensen EM ApE, a Plasmid Editor: A Freely Available DNA Manipulation and Visualization Program. Front. Bioinform 2022, 2, No. 818619. [PubMed: 36304290]

(35). Gietz RD; Schiestl RH High-Efficiency Yeast Transformation Using the LiAc/SS Carrier DNA/PEG Method. Nat. Protoc 2007, 2, 31–34. [PubMed: 17401334]

(36). Ito T; Tashiro K; Muta S; Ozawa R; Chiba T; Nishizawa M; Yamamoto K; Kuhara S; Sakaki Y Toward a Protein−Protein Interaction Map of the Budding Yeast: A Comprehensive System to Examine Two-Hybrid Interactions in All Possible Combinations between the Yeast Proteins. Proc. Natl. Acad. Sci 2000, 97, 1143–1147. [PubMed: 10655498]

(37). Guo Y; Cheng D; Lee TY; Wang J; Hsing I-M New Immunoassay Platform Utilizing Yeast Surface Display and Direct Cell Counting. Anal. Chem 2010, 82, 9601–9605. [PubMed: 21067137]

(38). Chan SK; Du P; Ignacio C; Mehta S; Newton IG; Steinmetz NF Biomimetic Virus-like Particles as Severe Acute Respiratory Syndrome Coronavirus 2 Diagnostic Tools. ACS Nano 2021, 15, 1259–1272. [PubMed: 33237727]

(39). Kajiwara K; Aoki W; Ueda M Evaluation of the Yeast Surface Display System for Screening of Functional Nanobodies. AMB Express 2020, 10, No. 51. [PubMed: 32180052]

(40). McMahon C; Baier AS; Pascolutti R; Wegrecki M; Zheng S; Ong JX; Erlandson SC; Hilger D; Rasmussen SGF; Ring AM; et al. Yeast Surface Display Platform for Rapid Discovery of Conformationally Selective Nanobodies. Nat. Struct. Mol. Biol 2018, 25, 289–296. [PubMed: 29434346]

(41). Chen M-H; Shen Z-M; Bobin S; Kahn PC; Lipke PN Structure of Saccharomyces Cerevisiae α-Agglutinin: Evidence for a Yeast Cell Wall Protein with Multiple Immunoglobulin-like Domains with Atypical Disulfides. J. Biol. Chem 1995, 270, 26168–26177. [PubMed: 7592821]

(42). Uchański T; Zögg T; Yin J; Yuan D; Wohlkönig A; Fischer B; Rosenbaum DM; Kobilka BK; Pardon E; Steyaert J An Improved Yeast Surface Display Platform for the Screening of Nanobody Immune Libraries. Sci. Rep 2019, 9, No. 382. [PubMed: 30674983]

(43). Palomares LA; Ramírez OT Challenges for the Production of Virus-like Particles in Insect Cells: The Case of Rotavirus-like Particles. Biochem. Eng. J 2009, 45, 158–167.

(44). Escudero-Abarca BI; Suh SH; Moore MD; Dwivedi HP; Jaykus L-A Selection, Characterization and Application of Nucleic Acid Aptamers for the Capture and Detection of Human Norovirus Strains. PLoS One 2014, 9, No. e106805. [PubMed: 25192421]

(45). Gao J; Zhang L; Xue L; Cai W; Qin Z; Yang J; Liang Y; Wang L; Chen M; Ye Q; et al. Development of a High-Efficiency Immunomagnetic Enrichment Method for Detection of Human Norovirus via PAMAM Dendrimer/SA-Biotin Mediated Cascade-Amplification. Front. Microbiol 2021, 12, 2049.

(46). Gupta N; Lainson JC; Belcher PE; Shen L; Mason HS; Johnston SA; Diehnelt CW Cross-Reactive Synbody Affinity Ligands for Capturing Diverse Noroviruses. Anal. Chem 2017, 89, 7174–7181. [PubMed: 28640636]

(47). Almand EA; Goulter RM; Jaykus L-A Capture and Concentration of Viral and Bacterial Foodborne Pathogens Using Apolipoprotein H. J. Microbiol. Methods 2016, 128, 88–95. [PubMed: 27439140]

(48). Jeong M-I; Park SY; Ha S-D Thermal Inactivation of Human Norovirus on Spinach Using Propidium or Ethidium Monoazide Combined with Real-Time Quantitative Reverse Transcription-Polymerase Chain Reaction. Food Control 2017, 78, 79–84.

(49). Herman KM; Hall AJ; Gould LH Outbreaks Attributed to Fresh Leafy Vegetables, United States, 1973−2012. Epidemiol. Infect 2015, 143, 3011–3021. [PubMed: 25697407]

(50). Ashiba H; Sugiyama Y; Wang X; Shirato H; Higo-Moriguchi K; Taniguchi K; Ohki Y; Fujimaki M Detection of Norovirus Virus-like Particles Using a Surface Plasmon Resonance-Assisted

Fluoroimmunosensor Optimized for Quantum Dot Fluorescent Labels. Biosens. Bioelectron 2017, 93, 260–266. [PubMed: 27597126]

(51). Chen J; Nugen SR Detection of Protease and Engineered Phage-Infected Bacteria Using Peptide-Graphene Oxide Nanosensors. Anal. Bioanal. Chem 2019, 411, 2487–2492. [PubMed: 30903224]

(52). Kitamoto N; Tanaka T; Natori K; Takeda N; Nakata S; Jiang X; Estes MK Cross-Reactivity among Several Recombinant Calicivirus Virus-like Particles (VLPs) with Monoclonal Antibodies Obtained from Mice Immunized Orally with One Type of VLP. J. Clin. Microbiol 2002, 40, 2459–2465. [PubMed: 12089262]

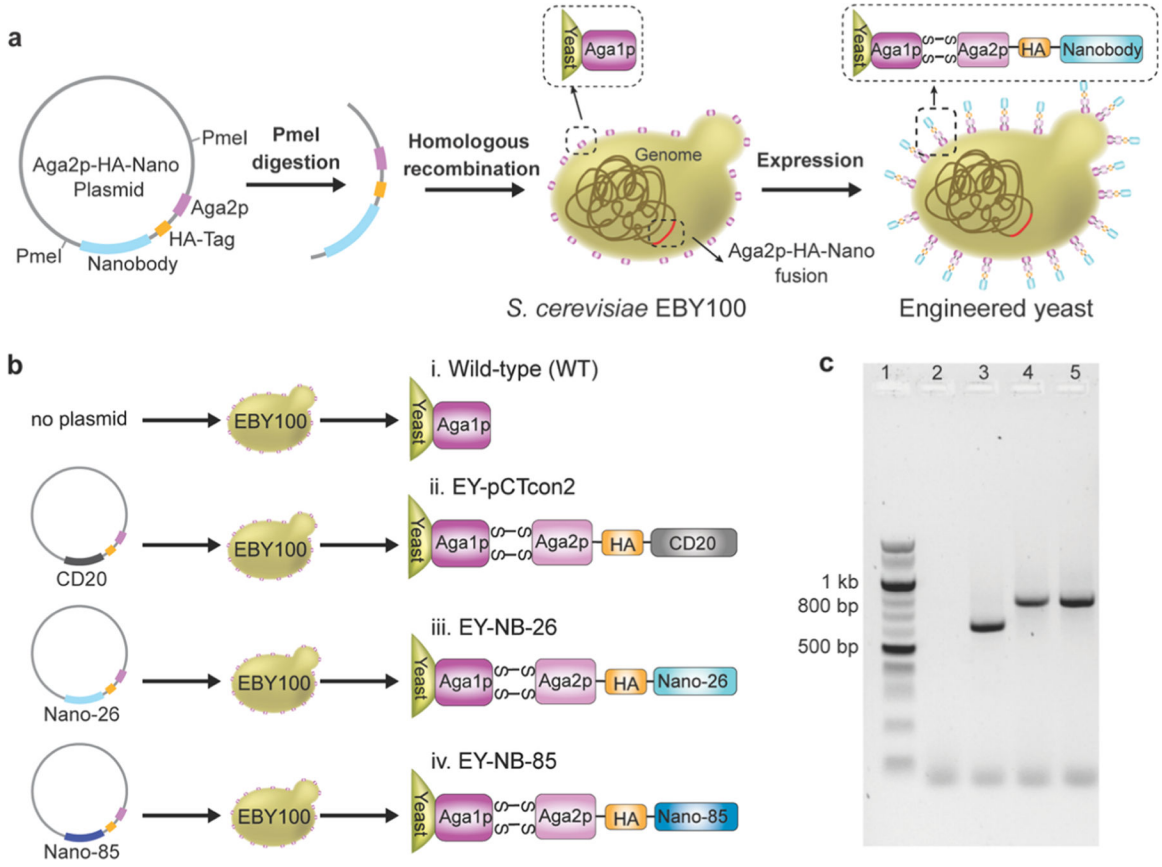

Figure 1.

(a) Schematic illustration of yeast surface engineering to display nanobody. (b) Construction of nanobody expression yeasts and their corresponding positions in the protein fusions. (c) Electrophoresis of yeast colony PCR for the verification of inserted Aga2p-HA-nanobody fusions. Lane 1, 100 bp DNA ladder; lane 2; wild-type; lane 3, EY-pCTcon2 (643 bp); lane 4, EY-NB-26 (814 bp); lane 5, EY-NB-85 (829 bp). Notes: EY, engineered yeast; NB, nanobody.

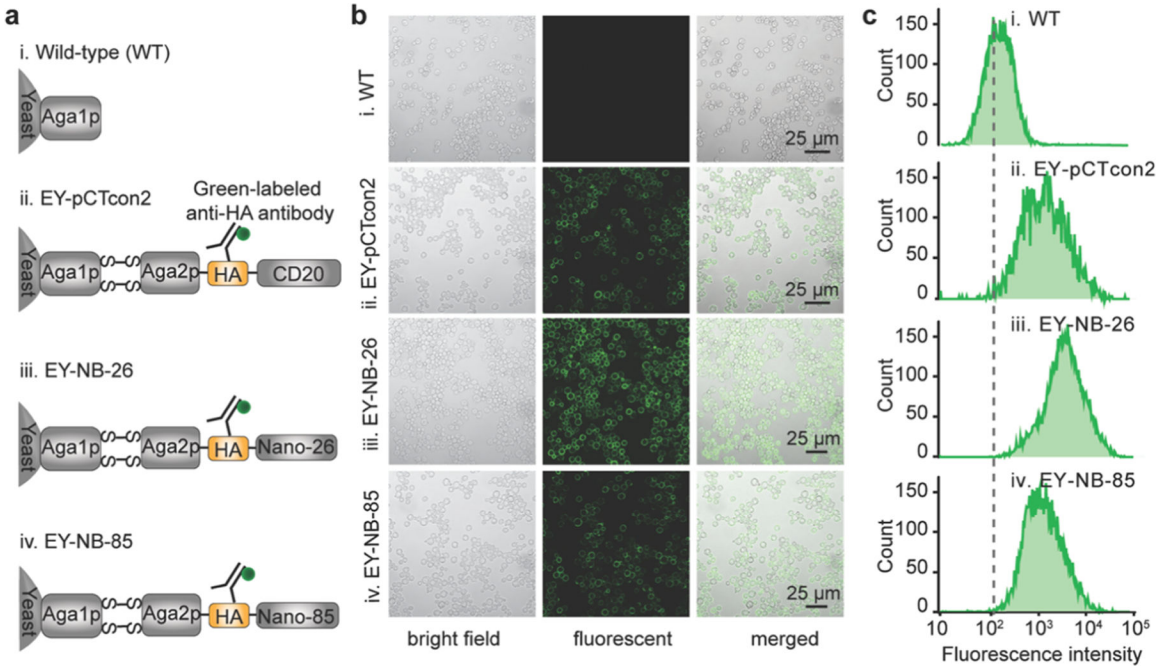

Figure 2.

(a) Schematic illustration of the Aga2p-HA-nanobody expression on the yeast surface. (b) Confocal images of fluorescence anti-HA antibody labeled yeast. (c) Histogram of the flow cytometric analysis of fluorescence anti-HA antibody labeled yeast. Notes: EY, engineered yeast; NB, nanobody.

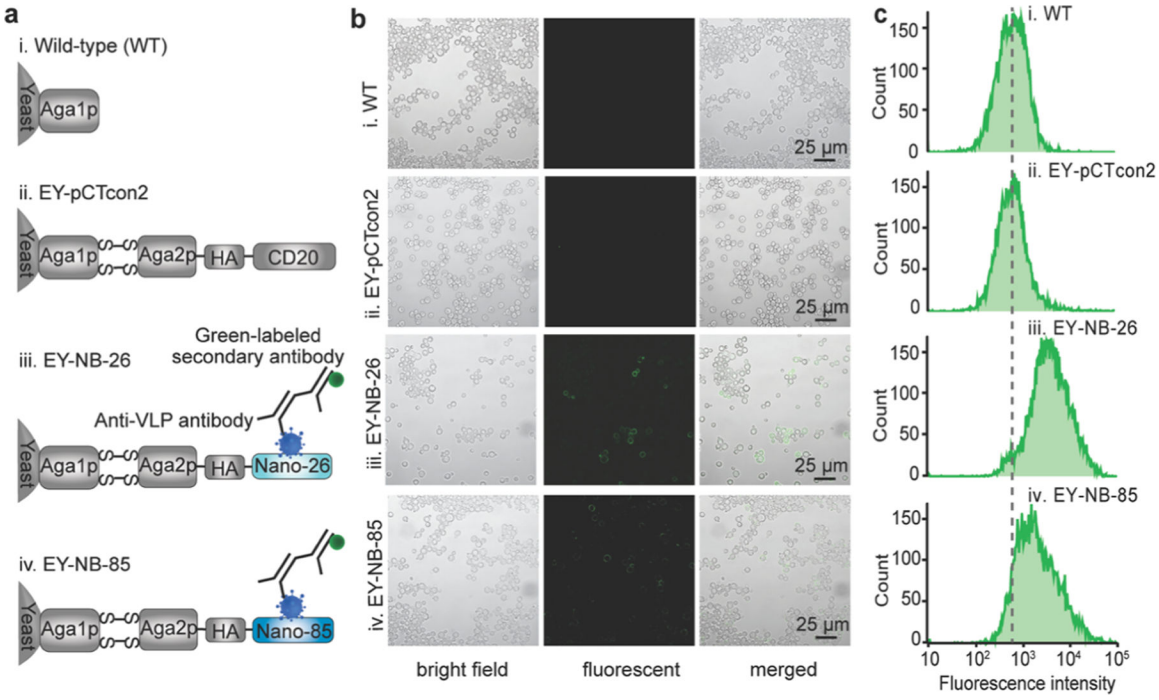

Figure 3.

(a) Schematic illustration of the norovirus VLP−nanobody binding. (b) Confocal images of the norovirus VLP−nanobody binding. (c) Histogram of the flow cytometric analysis of the norovirus VLP−nanobody binding.

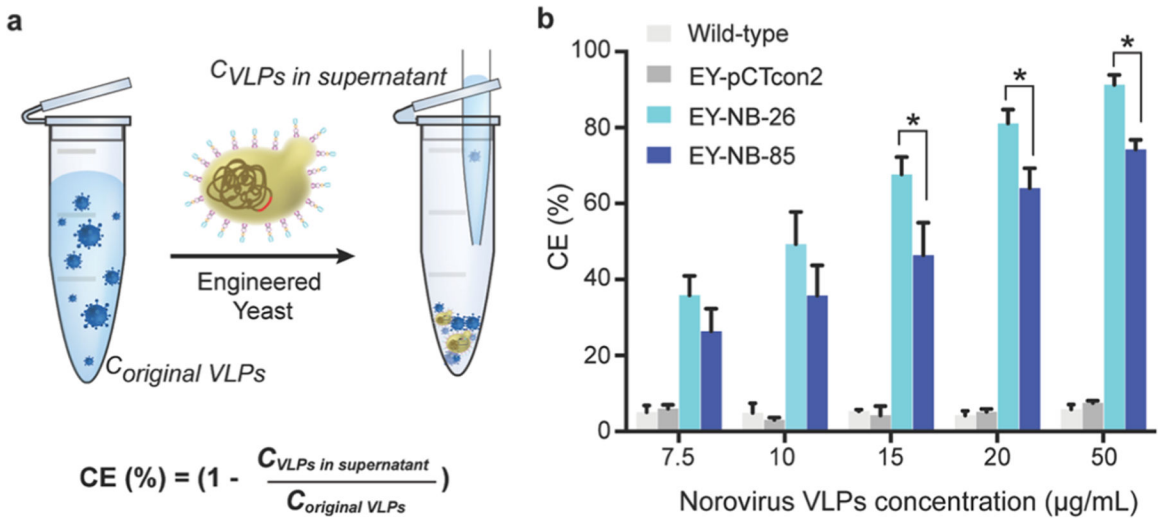

Figure 4.

(a) Schematic illustration of capture efficiency. (b) Comparison of capture efficiency among yeasts. Notes: EY, engineered yeast; NB, nanobody; CE, capture efficiency; VLP, virus-like particle.

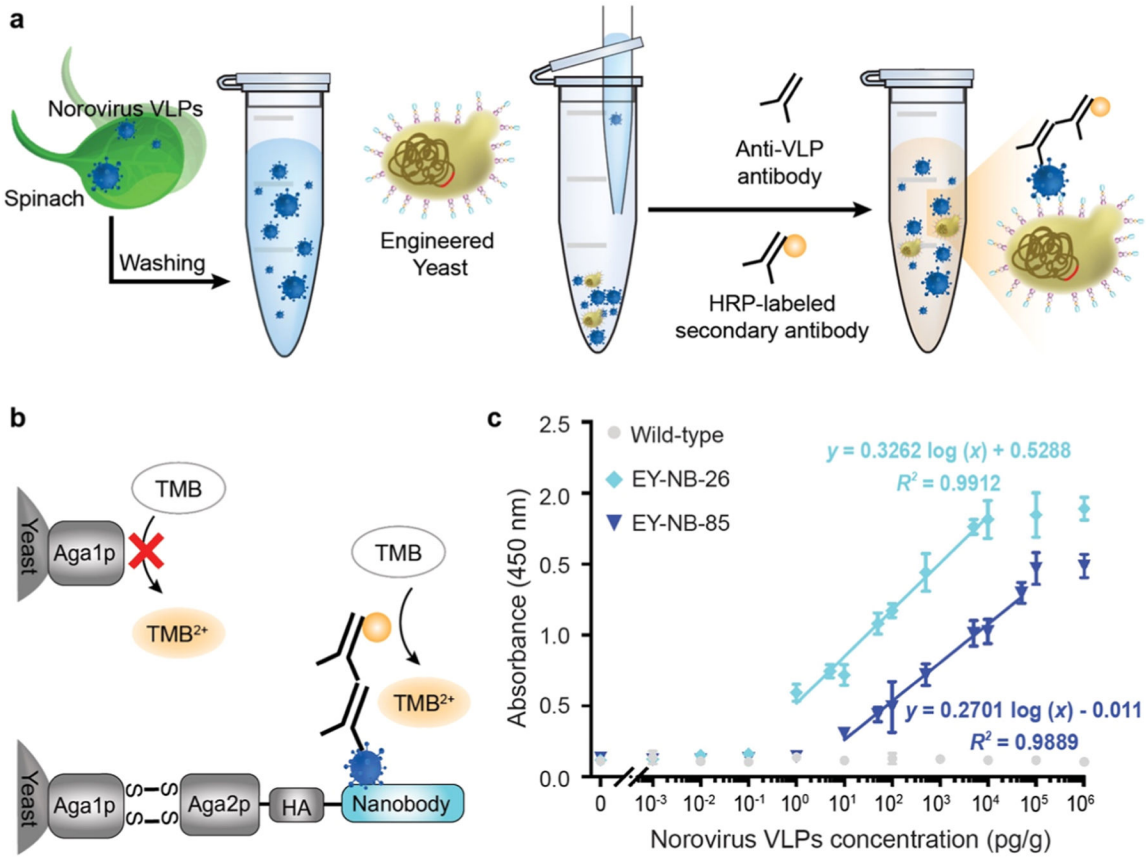

Figure 5.

(a) Concentration and detection of norovirus VLPs using engineered yeasts. (b) Comparison of wild-type and engineered yeasts for norovirus detection. (c) Absorbance intensity of norovirus detection using a sandwich assay. Notes: EY, engineered yeast; NB, nanobody; VLP, virus-like particle.